4-15-1985

Constraint on the optical constants of a film-substrate system for operation as an external-reflection retarder at a given angle of incidence

R. M.A. Azzam
University of New Orleans, razzam@uno.edu

Bruce E. Perilloux

Recommended Citation

R. M. A. Azzam and Bruce E. Perilloux, "Constraint on the optical constants of a film-substrate system for operation as an external-reflection retarder at a given angle of incidence," Appl. Opt. 24, 1171-1179 (1985)

Constraint on the optical constants of a film–substrate system for operation as an external-reflection retarder at a given angle of incidence

R. M. A. Azzam and Bruce E. Perilloux

Given a transparent film of refractive index n_1 on an absorbing substrate of complex refractive index n_2-jk_2, we examine the constraint on n_1, n_2, and k_2 such that the film–substrate system acts as an external-reflection retarder of specified retardance Δ at a specified angle of incidence ϕ. The constraint, which takes the form $f(n_1,n_2,k_2;\phi,\Delta) = 0$, is portrayed graphically by equi-n_1 contours in the n_2,k_2 plane at $\phi = 45, 70°$ and for $\Delta = \pm 90$ and $\pm 180°$, corresponding to quarterwave and halfwave retarders (QWR and HWR), respectively. The required film thickness as a fraction of the film thickness period and the polarization-independent device reflectance $\mathcal{R}$ are also studied graphically as functions of the optical constants. It is found that as $n_2 \to 0$, $\mathcal{R} \to 1$, so that a metal substrate such as Ag is best suited for high-reflectance QWR ($\phi > 45°$) and HWR ($\phi \leq 45°$). However, films that achieve QWR at $\phi \leq 45°$ are excellent antireflection coatings of the underlying dielectric, semiconductor, or metallic substrate.

I. Introduction

It has been shown[1–3] that, for a given optically isotropic system of a transparent thin film on an absorbing (or transparent) substrate, the p- and s-polarized components of incident monochromatic light can be reflected with equal attenuations and with a specified differential phase shift Δ; hence the system functions as an external-reflection retarder. This is achieved simply by selecting the proper angle of incidence ϕ and film thickness d.

This paper deals with such a film–substrate reflection retarder from a different and global point of view. Specifically, we consider the constraint on the optical constants of the film and substrate such that a specified retardance Δ is achieved at a given ϕ. The required film thickness as a fraction of the film thickness period, ζ, and the polarization-independent device reflectance (insertion loss), $\mathcal{R}$, are also computed. The results are presented graphically over a wide range of optical constants, without reference to a specific wavelength, for generality.

To keep the paper within reasonable bounds, we consider only two angles of incidence, $\phi = 45, 70°$ and two retardances $\Delta = \pm 90, \pm 180°$, corresponding to quarterwave and halfwave retarders (QWR and HWR), respectively. Results at other ϕ,Δ were obtained but are not given here. This paper also contains tables that give the characteristics of high-reflectance QWRs and HWRs using a thin-film-coated Ag substrate for several visible and near-IR wavelengths.

II. Basic Relations

The complex p- and s-reflection coefficients of a film–substrate system are[4]

$$R_\nu = (r_{01\nu} + r_{12\nu}X)/(1 + r_{01\nu}r_{12\nu}X), \quad \nu = p,s, \tag{1}$$

and their ratio

$$\rho = R_p/R_s \tag{2}$$

is given by

$$\rho = (A + BX + CX^2)/(D + EX + FX^2), \tag{3}$$

where

$$X = \exp(-j2\pi\zeta), \tag{4}$$

$$A = r_{01p}, \quad B = r_{12p} + r_{01p}r_{01s}r_{12s}, \quad C = r_{01s}r_{12p}r_{12s},$$

$$D = r_{01s}, \quad E = r_{12s} + r_{01p}r_{01s}r_{12p}, \quad F = r_{01p}r_{12p}r_{12s}. \tag{5}$$

In Eq. (4), ζ is the normalized film thickness,

$$\zeta = d/D_\phi, \tag{6}$$

where

The authors are with University of New Orleans, Department of Electrical Engineering, Lakefront, New Orleans, Louisiana 70148.

Received 9 October 1984.
0003-6935/85/081171-09$02.00/0.

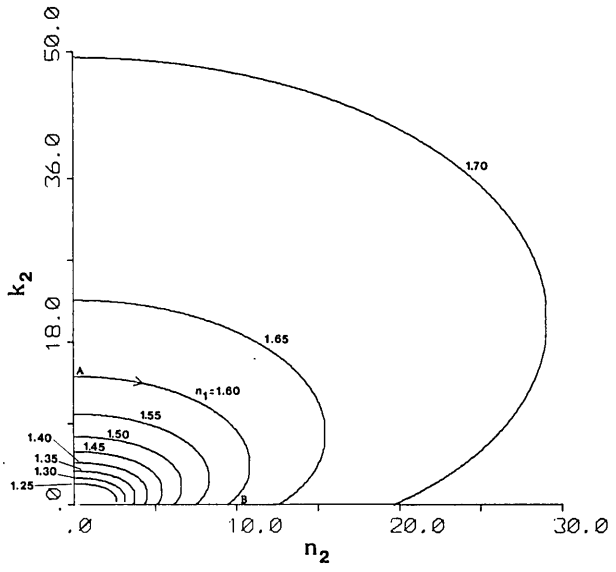

Fig. 1. Contours of constant film refractive index, n_1 = constant, in the n_2,k_2 plane, where n_2-jk_2 is the substrate complex refractive index. These equi-n_1 contours represent the constraint on the optical constants such that the ratio of the complex p- and s-reflection coefficients of the film–substrate system $\rho = j$ at $\phi = 70°$ angle of incidence, i.e., a quarterwave retarder (QWR) with p fast axis is realized.

$$D_\phi = \frac{\lambda}{2}(N_1^2 - N_0^2\sin^2\phi)^{-1/2} \tag{7}$$

is the film thickness period, and λ is the wavelength of light. N_0, N_1 (real), and N_2 (complex) are the refractive indices of the medium of incidence (0), film (1), and substrate (2), respectively. In Eqs. (1) and (5) $r_{ij\nu}$ denotes the (complex-amplitude) Fresnel reflection coefficient of the ij interface for the ν polarization. Such coefficients are given in standard optics texts.[5]

For simplicity, and without loss of generality, we define relative film and substrate refractive indices as follows:

$$N_1/N_0 = n_1, \qquad N_2/N_0 = n_2 - jk_2. \tag{8}$$

Often the medium of incidence is air ($N_0 = 1$) and the distinction between the relative and actual refractive indices disappears.

The constraint on n_1,n_2,k_2 such that a given ρ is realized at a given ϕ is obtained by solving Eq. (3) for X,

$$X = \frac{-(B - \rho E) \pm [(B - \rho E)^2 - 4(C - \rho F)(A - \rho D)]^{1/2}}{2(C - \rho F)}, \tag{9}$$

and requiring that

$$|X| = 1. \tag{10}$$

Equation (10) follows from Eqs. (4), (6), and (7), where we assume $N_1 > N_0 \sin\phi$, i.e., the absence of total internal reflection at the incidence medium–film interface.

Equation (10), where X is given by the right-hand side of Eq. (9), represents the desired constraint on the optical constants n_1, n_2, and k_2 for given ϕ and ρ. It can be put in the functional form

$$f(n_1,n_2,k_2;\phi,\rho) = 0. \tag{11}$$

With ϕ and ρ specified, Eq. (11) is represented graphically by contours of constant film refractive index (n_1 = constant) in the n_2,k_2 plane. To generate one such contour, n_1 is assigned a fixed value, n_2 is scanned over a certain range, and for each n_2 Eq. (11) is solved for k_2 as its only unknown by numerical iteration. Only positive k_2 values are sought and two roots may in general be obtained that correspond to the double roots of X (the $\pm$ signs) in Eq. (9). That a proper root has been found is verified by substituting n_1,n_2,k_2,ρ,ϕ into the right-hand side of Eq. (9) and checking that

$$|X| - 1 < 10^{-6}. \tag{12}$$

The required normalized film thickness ζ is obtained from complex X via Eq. (4),

$$\zeta = -\arg(X)/2\pi. \tag{13}$$

The proper multiple of 2π is added to $\arg X$, so that ζ is in the reduced range

$$0 < \zeta < 1. \tag{14}$$

The device reflectance is computed from Eq. (1),

$$\mathcal{R}_\nu = |R_\nu|^2, \tag{15}$$

and is ascertained to be the same for the $\nu = p$ and $\nu = s$ polarizations.

As indicated in Sec. I, we limit ourselves to film–substrate external-reflection quarterwave and halfwave retarders, $\rho = \pm j$ (QWR) and $\rho = -1$ (HWR) at two angles of incidence $\phi = 70°$ and $\phi = 45°$. Only n_1 values >1 are taken (i.e., the film is assumed to be more optically dense than the medium of incidence), and, with one exception, we restrict ourselves to a square of side 10 in the n_2,k_2 plane (i.e., $0 \le n_2 \le 10$, $0 \le k_2 \le 10$). This corresponds to most substrate materials in the NUV–VIS–NIR spectral range. The n_1 values are selected to generate reasonably well-spaced equi-n_1 contours in the n_2,k_2 plane.

III. Quarterwave and Halfwave Retarders at 70° Angle of Incidence

A. $\rho = +j$ QWR

Let us first consider $\rho = j$, which corresponds to a QWR with p fast axis[6] (i.e., parallel to the plane of incidence) at $\phi = 70°$. Figure 1 shows a family of ten equi-n_1 contours in the n_2,k_2 plane, for n_1 values (marked by each curve) from 1.25 to 1.70 in equal steps of 0.05. This is the only case where we allowed n_2 and k_2 to assume values >10. (The extended rectangular range $0 \le n_2 \le 30$, $0 \le k_2 \le 50$ covers the optical constants of metals beyond the near and into the middle IR spectrum.) Refractive indices in the range $1.25 \le n_1 \le 1.70$ correspond to several existing thin-film coating materials,[7,8] so that this $\phi = 70°$ QWR is readily realizable with many film–substrate combinations at different wavelengths, with light incident from air or vacuum.

Figure 2 shows the variation of the normalized film thickness ζ (required to achieve QWR at $\phi = 70°$) along

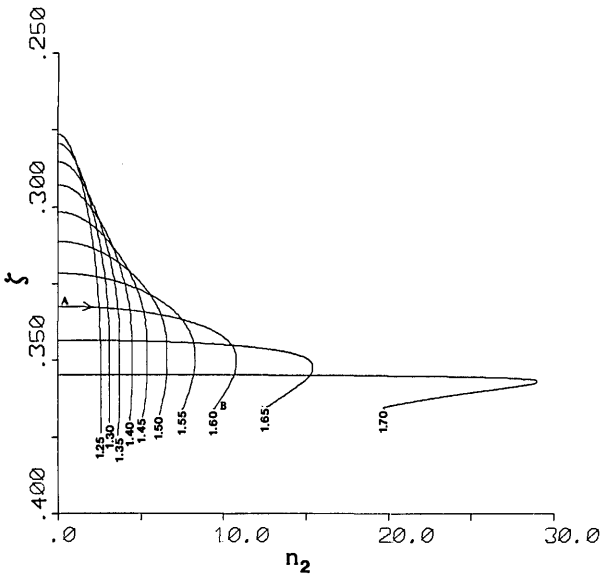

Fig. 2. Film thickness as a fraction of the film thickness period ζ, required to achieve $\rho = j$ QWR at $\phi = 70°$, plotted as a function of n_2 at constant n_1 (marked by each curve). n_1,n_2 specify a particular film–substrate QWR completely, because k_2 can be deduced from Fig. 1. The contour AB describes the variation of ζ with n_2 along the similarly marked $n_1 = 1.6$ contour in Fig. 1.

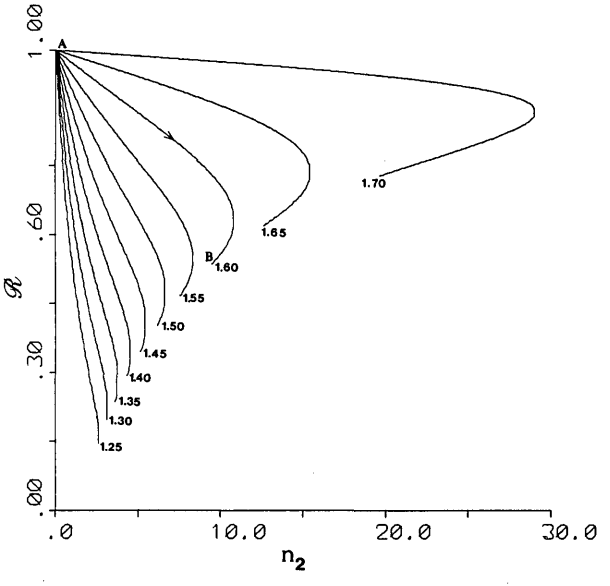

Fig. 3. Polarization-independent reflectance $\mathcal{R}$ of film–substrate $\rho = j$ QWRs at $\phi = 70°$ plotted as a function of n_2 at constant n_1 (marked by each curve) along the equi-n_1 contours of Fig. 1.

each and every one of the n_1 = constant contours of Fig. 1. The $n_1 = 1.6$ contour has been marked by its end points A and B in Figs. 1 and 2 [and 3] and by an arrow pointing from A to B. In Fig. 1 points A and B represent the limiting states of the substrate being perfectly metallic ($n_2 = 0$) and perfectly dielectric ($k_2 = 0$), respectively. As a point moves along the $n_1 = 1.6$ contour from A to B in Fig. 1, ζ varies (increases monotonically) from ζ_A to ζ_B along the corresponding ($n_1 = 1.6$) contour of Fig. 2. It is significant to note that ζ occupies only a narrow range, $0.275 < \zeta < 0.375$, for all $\rho = j$ QWRs at $\phi = 70°$. represented in Fig. 1.

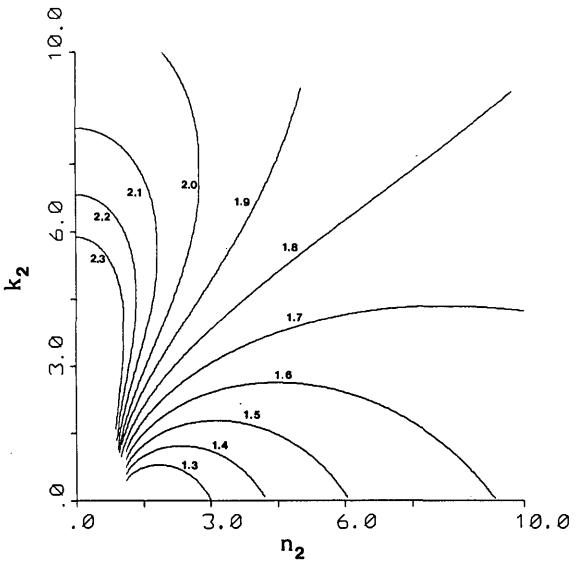

Fig. 4. Same as Fig. 1 except that $\rho = -j$ (QWR with s fast axis).

Figure 3 describes the variation with n_2 of the reflectance $\mathcal{R}$ (which is the same for the p and s polarizations) along each and every n_1 = constant contour of Fig. 1. In Figs. 2 and 3 an (n_1,n_2) pair defines one device completely, because k_2 can be obtained from Fig. 1. It is evident from Fig. 3 that $\mathcal{R} = 1$ when $n_2 = 0$, hence an ideal, lossless (total-reflection) QWR is obtained. This most desirable characteristic can be very nearly achieved by using a metallic substrate such as Ag[9] in the visible and near IR, as will be demonstrated in Sec. V. Movement along any equi-n_1 contour in Fig. 1 from the $n_2 = 0$ point (such as A) to the $k_2 = 0$ point (such as B) is accompanied by a monotonic decrease of the reflectance $\mathcal{R}$ from a maximum of 1 to a certain minimum $\mathcal{R}_m$ that depends on n_1. $\mathcal{R}_m$, hence the device reflectance in general, increases as n_1 is increased. It is also evident from Fig. 1 that higher values of the film refractive index n_1 are associated with higher substrate optical constants n_2, k_2, or higher $(n_2^2 + k_2^2)^{1/2}$ in particular.

B. $\rho = -j$ QWR

The case of $\rho = -j$ represents a QWR with the fast axis in the s direction (perpendicular to the plane of incidence). Again we take $\phi = 70°$.

Figure 4 shows a family of equi-n_1 contours, corresponding to n_1 from 1.3 to 2.3 in equal steps of 0.1, in the n_2,k_2 plane. (From now on, n_2 and k_2 are limited to a maximum of 10.) All curves appear to emanate from the point $n_2 = 1$, $k_2 = 0$. Contours that correspond to $n_1 \leq 1.7$ terminate on the n_2 axis ($k_2 = 0$), whereas those for $n_1 \geq 1.8$ terminate on the k_2 axis ($n_2 = 0$). Again with an air or vacuum ambient this range of n_1 corresponds to a variety of suitable thin-film coating materials,[7,8] so that $\rho = -j$ QWRs are readily realizable.

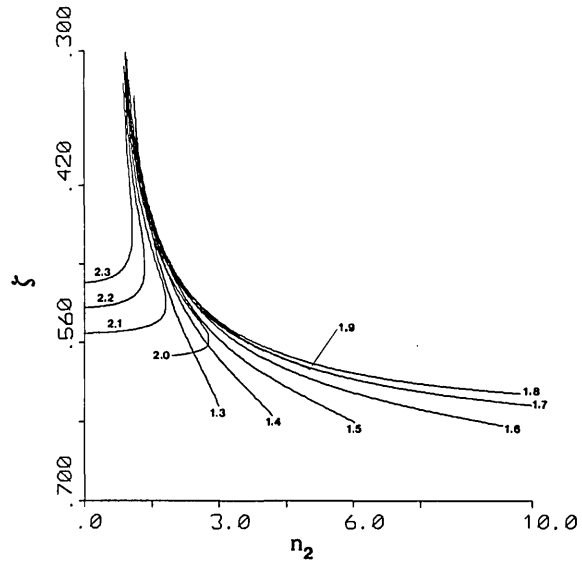

Fig. 5. Same as Fig. 2 except that $\rho = -j$ (QWR with s fast axis).

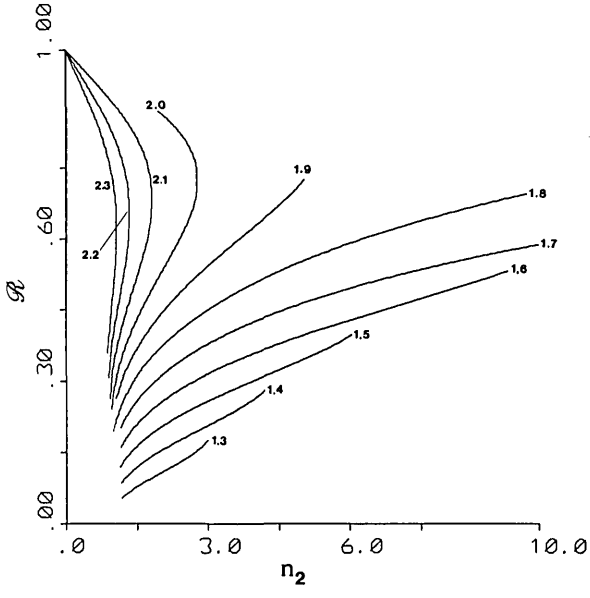

Fig. 6. Same as Fig. 3 except that $\rho = -j$ (QWR with s fast axis).

Figure 5 gives the associated normalized film thickness ζ and Fig. 6 the corresponding device reflectance $\mathcal{R}$. As before, a particular device is completely specified by (n_1,n_2), because k_2 is determined from Fig. 4.

Comparing Figs. 3 and 6 we find that, for films of $n_1 \leq 1.7$, reflectance is generally lower for the $\rho = -j$ QWR than it is for the $\rho = j$ QWR at the same ($\phi = 70°$) angle of incidence. (Of course, the associated n_2,k_2 domains are different in both cases.) Nearly ideal total-reflection ($\mathcal{R} = 1$), $\rho = -j$, QWRs are attainable with high-index ($n_1 > 1.8$) films on (metallic) substrates with $n_2 \simeq 0$ such as Ag. The situation when $n_2 = 0$ is similar to that encountered in total internal reflection (TIR) at dielectric–dielectric interfaces. Although a differential phase shift and equal unity reflectances are attained with a film-free interface, the application of thin films of appropriate index and thickness allows the

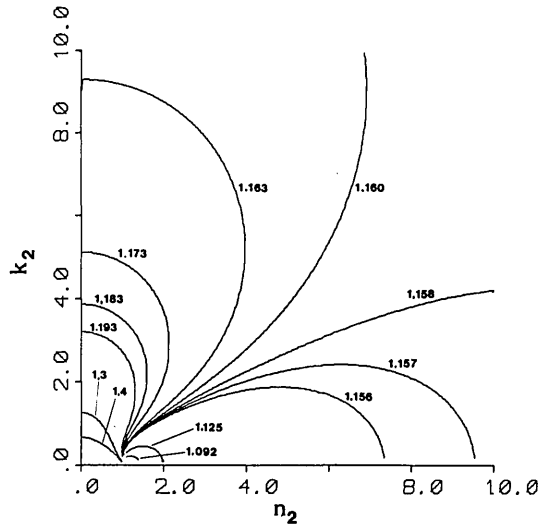

Fig. 7. Same as Fig. 1 except that $\rho = -1$, corresponding to halfwave retarders (HWR), also at $\phi = 70°$.

adjustment of the retardance Δ to a desired value[10] (such as $\pm 90°$) at a specified angle.

C. HWR

The third case to be considered at $\phi = 70°$ is that of $\rho = -1$, i.e., a halfwave retarder. Figure 7 shows the equi-n_1 contours in the n_2,k_2 plane for nonuniformly spaced n_1 values from 1.092 to 1.4. It is evident that the constraint on n_1,n_2,k_2 to achieve $\rho = -1$ at $\phi = 70°$ is very sensitive to small changes of n_1 ($\Delta n_1 = 0.001$) around $n_1 = 1.1$. All curves emanate from the point $n_2 = 1$, $k_2 = 0$ and terminate either on the n_2 or the k_2 axis. Data for $n_1 < 1.3$ are meaningful only if a dense medium of incidence ($N_0 > 1$) is assumed (which may serve as the substrate if it is a solid phase). For light incident from vacuum or air, HWRs at $\phi = 70°$ require films with $n_1 > 1.3$ on substrates with $n_2 < 1$ and $k_2 < 2$. The latter optical constants are typical of some metals in the UV.[11]

Figures 8 and 9 show the variation of ζ and $\mathcal{R}$, respectively, with n_2 along each and every n_1 = constant contour in Fig. 7. In Fig. 8 it appears that $\zeta \to 0$ as $n_2 \to 1$. In Fig. 9 we see that, for $n_1 > 1.16$, $\mathcal{R} = 1$ at $n_2 = 0$; this represents totally reflecting HWRs at $\phi = 70°$. Note also that, for $n_1 \geq 1.3$, $\mathcal{R}$ decreases steeply from 1 to 0 as n_2 increases from 0 to 1.

IV. Quarterwave and Halfwave Retarders at 45° Angle of Incidence

We now present and briefly discuss the results obtained when the procedure of Sec. II is applied with $\rho = j$ (QWR, p fast axis), $\rho = -j$ (QWR, s fast axis), and $\rho = -1$ (HWR) at $\phi = 45°$ as another (perhaps more attractive) angle of incidence.

The $\rho = j$ QWR is illustrated by Figs. 10, 11, and 12 which show the equi-n_1 contours in the n_2,k_2 plane, ζ vs n_2 at constant n_1, and $\mathcal{R}$ vs n_2 at constant n_1, respectively.

The $\rho = -j$ QWR is represented by Figs. 13–15 in the same fashion.

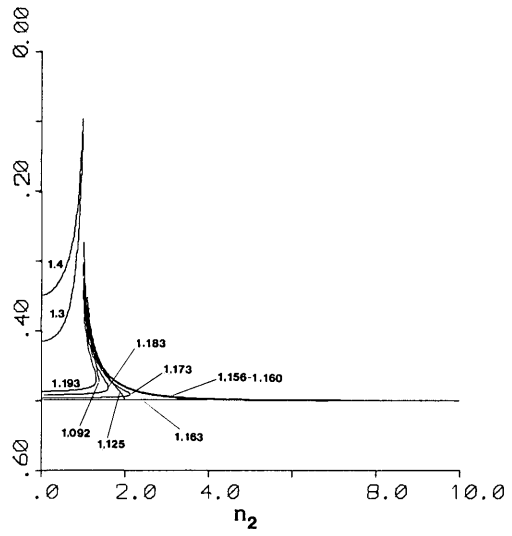

Fig. 8. Same as Fig. 2 except that $\rho = -1$ (HWR).

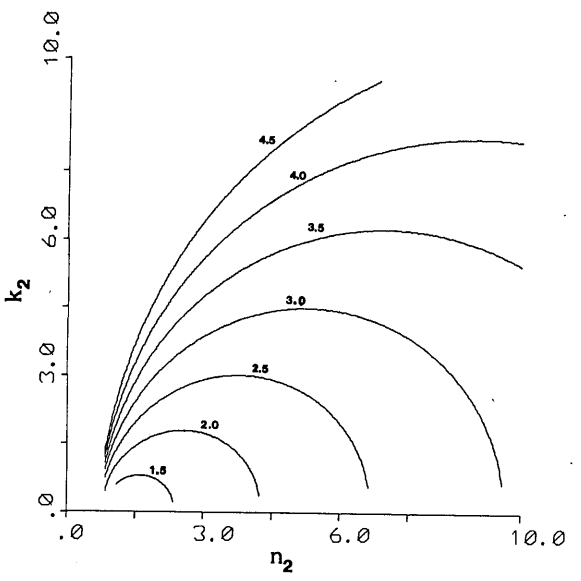

Fig. 10. Equi-n_1 contours in the n_2,k_2 plane for $\rho = j$ (QWR, p fast axis) at $\phi = 45°$ angle of incidence.

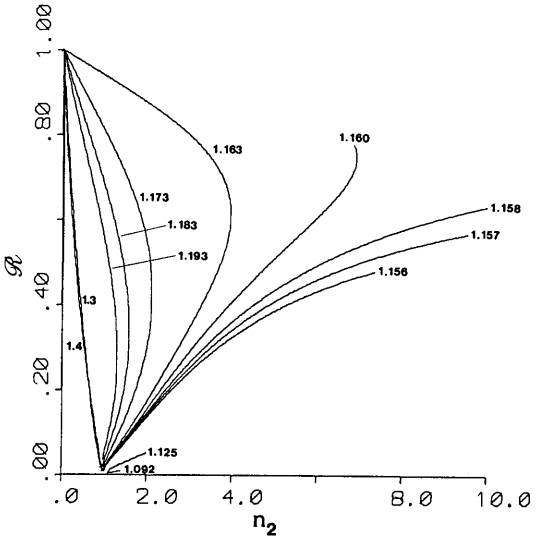

Fig. 9. Same as Fig. 3 except that $\rho = -1$ (HWR).

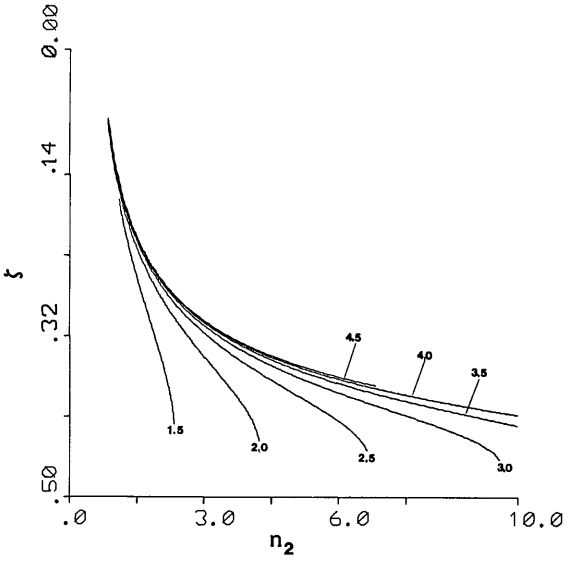

Fig. 11. Normalized film thickness ζ as a function of n_2 at constant n_1 (marked by each curve) corresponding to the data of Fig. 10 for $\rho = j$ (QWR, p fast axis) at $\phi = 45°$.

These graphical results should now be self-explanatory in view of the 70° cases already discussed in Sec. III.

The most remarkable observation is that the reflectance $\mathcal{R}$, which is the same for the p and s (hence for all incident) polarizations, becomes very low (<7% in all cases). Consequently, the film that produces QWR is also an efficient antireflection coating at 45°, especially with $n_1 < 2$. This is portrayed by Figs. 12 and 15, which also indicate that lower reflectances accompany the −90° rather than the +90° retardance. What adds to the importance of these (and other) results is the global way in which a vast range of substrates and films is considered.

Finally, Figs. 16–18 illustrate HWRs ($\rho = -1$) at $\phi =$ 45°. Compared with HWRs that we obtained earlier at $\phi = 70°$ (Figs. 7–9), HWRs at $\phi = 45°$ can be constructed from many combinations of films and substrates with refractive indices covering wide and realistic ranges and with the medium of incidence conveniently being air or vacuum.

Figure 17 shows that the normalized film thickness ζ required to achieve $\rho = -1$ at $\phi = 45°$ is between 0 and 0.5.

In Fig. 18 we observe that high reflectance $\mathcal{R}$ (approaching 100%) is again achieved when $n_2 \ll 1$. This is further demonstrated in Sec. V which provides data on HWRs at $\phi = 45°$ using a Ag substrate at several wavelengths in the visible and near IR.

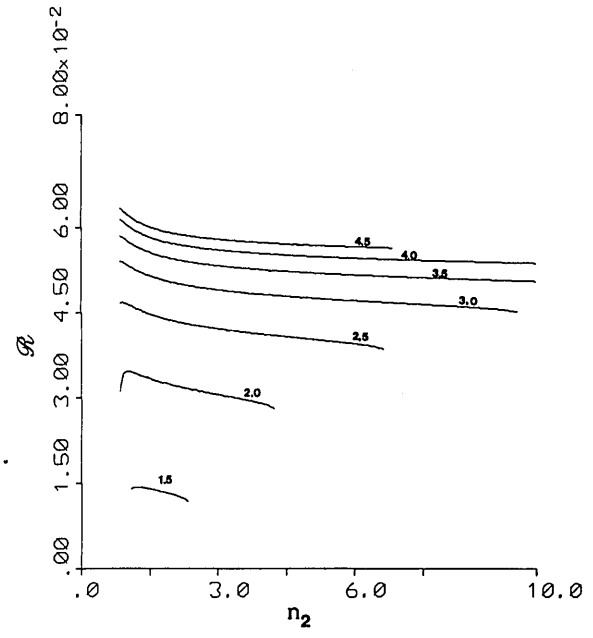

Fig. 12. Polarization-independent reflectance $\mathcal{R}$ as a function of n_2 at constant n_1 (marked by each curve) corresponding to the data of Fig. 10 for $\rho = j$ (QWR, p fast axis) at $\phi = 45°$.

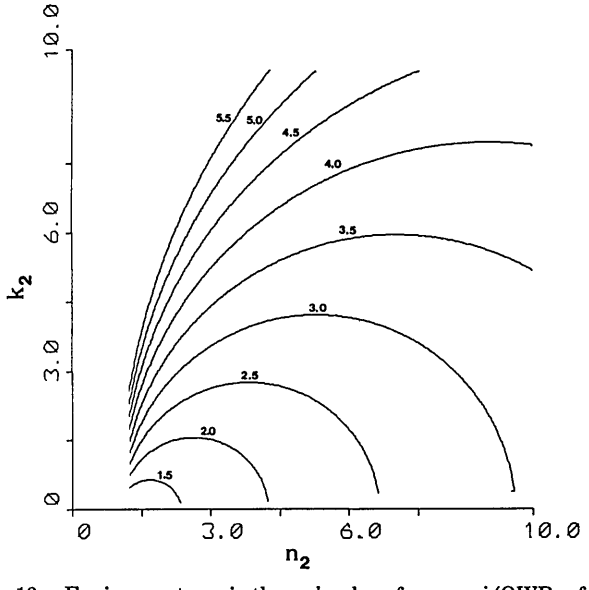

Fig. 13. Equi-n_1 contours in the n_2,k_2 plane for $\rho = -j$ (QWR, s fast axis) at $\phi = 45°$.

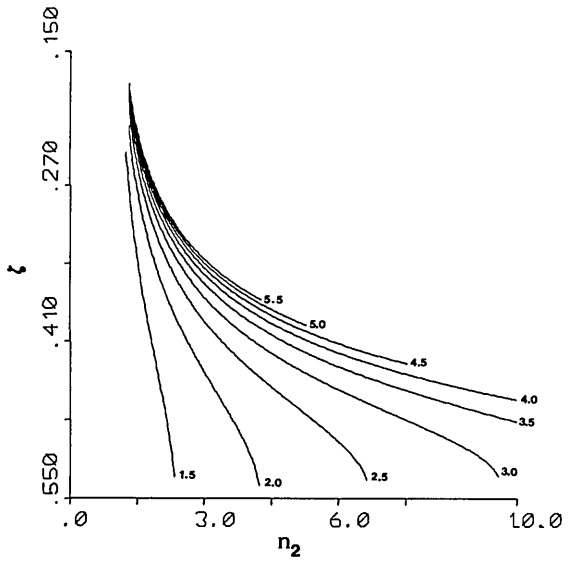

Fig. 14. Normalized film thickness ζ as a function of n_2 at constant n_1 (marked by each curve) corresponding to the data of Fig. 13 for $\rho = -j$ (QWR, s fast axis) at $\phi = 45°$.

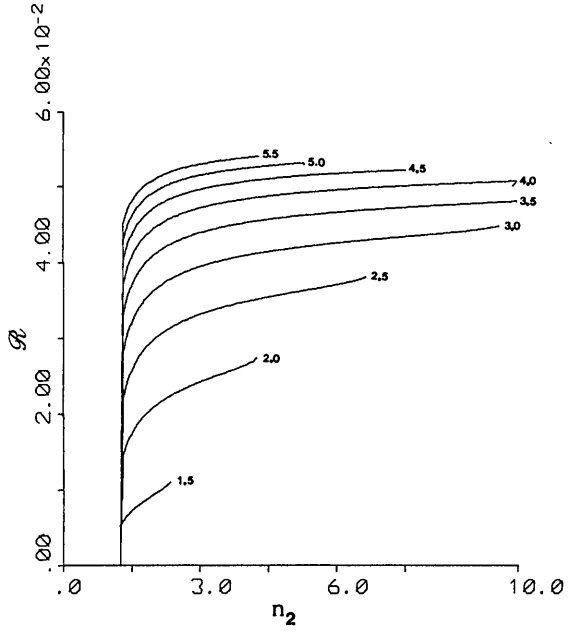

Fig. 15. Polarization-independent reflectance $\mathcal{R}$ as a function of n_2 at constant n_1 (marked by each curve) corresponding to the data of Fig. 13 for $\rho = -j$ (QWR, s fast axis) at $\phi = 45°$.

V. Quarterwave and Halfwave Retarders Using a Ag Substrate Coated by a Dielectric Thin Film

So far we have kept general our discussion of the constraint on n_1,n_2,k_2 such that a film–substrate system functions as an external-reflection retarder with specified retardance at a specified angle of incidence. Figures 1–18 are applicable to a wide range of ambient, film, and substrate materials and over a wide range of wavelengths. However, we have already remarked in Secs. III and IV that a high-reflectance metal substrate, such as Ag, would be ideally suited for high-reflectance devices[12]. In this section we present specific examples of Ag-based QWRs and HWRs in the visible and near IR, and we examine their sensitivity to small errors of incidence angle and of film refractive index and thickness. The assumed optical constants n_2,k_2 of Ag are those cited in Ref. 9.

To obtain the required film characteristics, the sequence of calculations is altered slightly from what we indicated in the discussion following Eq. (11). Here the substrate optical constants n_2,k_2 (and ρ,ϕ) are specified

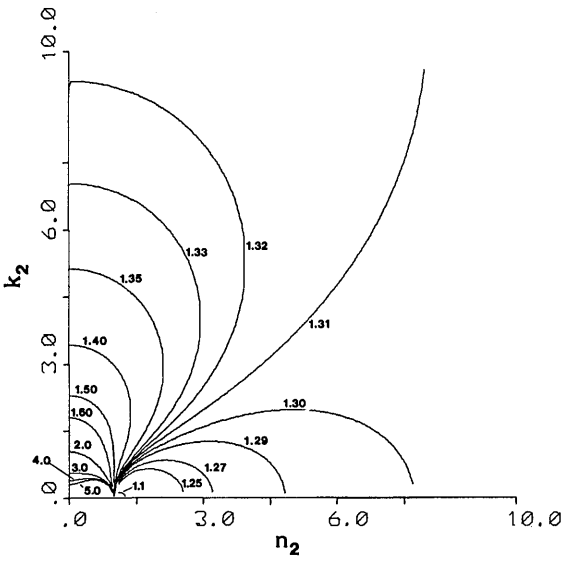

Fig. 16. Equi-n_1 contours in the n_2,k_2 plane for $\rho = -1$ halfwave retarders (HWR) at $\phi = 45°$ angle of incidence.

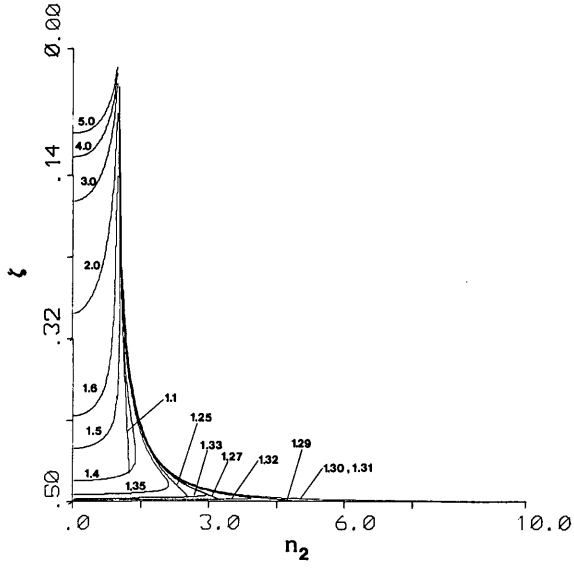

Fig. 17. Normalized film thickness ζ as a function of n_2 at constant n_1 (marked by each curve) corresponding to the data of Fig. 16 for $\rho = -1$ (HWR) at $\phi = 45°$.

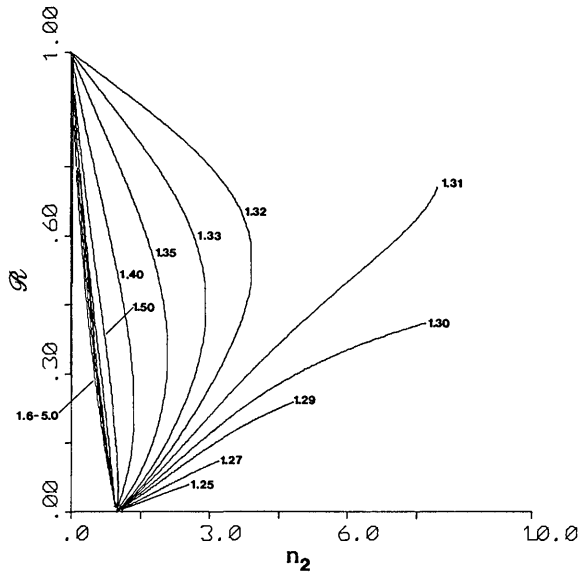

Fig. 18. Polarization-independent reflectance $\mathcal{R}$ as a function of n_2 at constant n_1 (marked by each curve) corresponding to the data of Fig. 16 for $\rho = -1$ (HWR) at $\phi = 45°$.

and Eq. (11) is solved for n_1 as its only unknown by iteration. Subsequently, the normalized and actual film thicknesses (ζ,d) and the device reflectance ($\mathcal{R}$) are computed as before.

Table I gives the characteristics of $\rho = +j$ QWRs for $\phi = 70°$ at several wavelengths. The required refractive index n_1, normalized thickness ζ, and actual thickness d (nm) of the thin dielectric film on Ag are all listed. The polarization-independent device reflectance, which appears in the last column of Table I, exceeds 97% at all wavelengths ≥500 nm.

We have also examined the effect of small errors of (a) angle of incidence ($\Delta\phi = 0.1°$), (b) film refractive index ($\Delta n_1 = 0.01$), and (c) film thickness ($\Delta d = 1$ nm) on the device performance as represented by the ratio ρ of the complex p- and s-reflection coefficients. Specifically, we have calculated the magnitude error $|\rho| - 1$, and phase error $(\arg\rho) - \Delta_{nom}$, where Δ_{nom} is the nominal retardance in degrees ($\Delta_{nom} = 90°$ for the $\rho = +j$ QWR, and $\Delta_{nom} = \pm 180°$ for the HWR). The results are listed in Table II. All errors fall within rea-

Table I. Characteristics of Quarterwave Retarders (QWR, $\rho = +j$) at 70° Angle of Incidence Using a Dielectric Thin Film on a Ag Substrate at Several Wavelengths [a]

λ(nm)	n_2	k_2	n_1	ζ	d(nm)	$\mathcal{R}$(%)
400	0.075	1.93	1.219154	0.277011	71.33	94.09
500	0.050	2.87	1.291322	0.278893	78.72	97.72
600	0.060	3.75	1.349785	0.285499	88.39	98.20
700	0.075	4.62	1.396728	0.292587	99.10	98.40
800	0.090	5.45	1.433078	0.298824	110.48	98.55
950	0.110	6.56	1.471883	0.306027	128.32	98.72
2000	0.480	14.40	1.601287	0.332817	256.69	98.69

[a] λ is the wavelength of light. n_2,k_2 are the real and imaginary parts of the Ag substrate complex refractive index (from Ref. 9). n_1 is the film refractive index obtained by solving Eq. (11) with $\rho = +j$ and $\phi = 70°$. ζ and d are the normalized and actual (least) film thicknesses, respectively, and $\mathcal{R}$ is the polarization-independent reflectance of the QWR.

Table II. Absolute Values of the Magnitude Error ($|\rho| - 1$) and Phase Error ($\arg\rho - 90°$) Caused by Introducing, One at a Time, an Angle-of-Incidence Error $\Delta\phi = 0.1°$, a Film-Refractive-Index Error $\Delta n_1 = 0.01$, or a Film-Thickness Error $\Delta d = 1$ nm to the QWR Designs at $\phi = 70°$ Listed in Table I

	$\Delta\phi = 0.1°$		$\Delta n_1 = 0.01$		$\Delta d = 1$ nm	
λ(nm)	Magnitude error	Phase error (deg)	Magnitude error	Phase error (deg)	Magnitude error	Phase error (deg)
400	0.37×10^{-4}	0.329	0.198×10^{-2}	2.004	0.613×10^{-3}	1.246
500	0.61×10^{-5}	0.341	0.066×10^{-2}	1.044	0.298×10^{-3}	0.961
600	0.19×10^{-5}	0.344	0.047×10^{-2}	0.681	0.245×10^{-3}	0.773
700	0.31×10^{-6}	0.345	0.038×10^{-2}	0.506	0.214×10^{-3}	0.645
800	0.49×10^{-6}	0.345	0.033×10^{-2}	0.414	0.186×10^{-3}	0.553
950	0.10×10^{-5}	0.345	0.028×10^{-2}	0.335	0.151×10^{-3}	0.457
2000	0.25×10^{-5}	0.345	0.024×10^{-2}	0.185	0.093×10^{-3}	0.214

Table III. Characteristics of Halfwave Retarders (HWR) at 45° Angle of Incidence Using a Dielectric Thin Film on a Ag Substrate at Several Wavelengths [a]

λ(nm)	n_2	k_2	n_1	ζ	d(nm)	$\mathcal{R}$(%)
400	0.075	1.93	1.566251	0.417418	59.74	90.89
500	0.050	2.87	1.436138	0.464840	92.97	96.51
600	0.060	3.75	1.385496	0.481921	121.35	97.36
700	0.075	4.62	1.359636	0.489611	147.57	97.76
800	0.090	5.45	1.345145	0.493407	172.49	98.03
950	0.110	6.56	1.333442	0.496091	208.45	98.31
2000	0.480	14.40	1.312227	0.499608	451.99	98.44

[a] λ is the wavelength of light. n_2,k_2 are the real and imaginary parts of the Ag substrate complex refractive index (from Ref. 9). n_1 is the film refractive index obtained by solving Eq. (11) with $\rho = -1$ and $\phi = 45°$. ζ and d are the normalized and actual (least) film thicknesses, respectively, and $\mathcal{R}$ is the polarization-independent reflectance of the HWR.

Table IV. Absolute Values of the Magnitude Error ($|\rho| - 1$) and Phase Error ($\arg\rho - 180°$) Caused by Introducing, One at a Time, an Angle-of-Incidence Error $\Delta\phi = 0.1°$, a Film-Refractive-Index Error $\Delta n_1 = 0.01$, or a Film-Thickness Error $\Delta d = 1$ nm to the HWR Designs at $\phi = 45°$ Listed in Table III

	$\Delta\phi = 0.1°$		$\Delta n_1 = 0.01$		$\Delta d = 1$ nm	
λ(nm)	Magnitude error	Phase error (deg)	Magnitude error	Phase error (deg)	Magnitude error	Phase error (deg)
400	0.469×10^{-4}	0.018	0.512×10^{-3}	0.977	0.101×10^{-2}	0.959
500	0.186×10^{-4}	0.003	0.116×10^{-3}	1.130	0.207×10^{-3}	0.716
600	0.138×10^{-4}	0.016	0.398×10^{-4}	1.179	0.101×10^{-3}	0.592
700	0.113×10^{-3}	0.024	0.291×10^{-5}	1.188	0.604×10^{-4}	0.509
800	0.956×10^{-5}	0.029	0.169×10^{-4}	1.181	0.396×10^{-4}	0.446
950	0.781×10^{-5}	0.035	0.306×10^{-4}	1.163	0.239×10^{-4}	0.377
2000	0.586×10^{-5}	0.048	0.682×10^{-4}	1.058	0.506×10^{-5}	0.182

sonable limits, so that these QWRs are not overly sensitive to changes of the different design parameters.

Table III shows the characteristics of HWRs operating at the (desirable) incidence angle of 45° and at the same wavelengths selected in Table I. Note that $\mathcal{R} >$ 96% for all $\lambda \geq 500$ nm, indicating an efficient device. The magnitude and phase errors that result from (a) $\Delta\phi = 0.1°$ angle-of-incidence error, (b) $\Delta n_1 = 0.01$ film-refractive-index error, and (c) $\Delta d = 1$ nm film-thickness error are all listed in Table IV. Again, the errors fall within reasonable limits so that good, but not very stringent, control on film deposition is required. Particularly noticeable in Table IV is the negligible sensitivity to incidence-angle errors. This is expected from Ref. 3, which indicates that such HWRs would continue to operate as HWRs from normal incidence to and beyond the design angle of 45°.

A wide selection of thin-film coating materials is available[7,8] with the requisite refractive indices listed in the fourth column of Tables I and III.

VI. Summary

Comprehensive results have been presented of film–substrate QWR and HWR at 70° and 45° angles of incidence. The constraint on the optical constants of the film (n_1) and substrate (n_2,k_2), such that a given ratio ρ of the complex p and s reflection is achieved at a given angle of incidence, is elucidated with graphs showing equi-n_1 contours in the n_2,k_2 plane for $\rho = \pm j$ (QWR) and $\rho = -1$ (HWR). The required film thickness as a fraction of the film thickness period and the polarization-independent device reflectance are also studied graphically as functions of the optical constants. Films that achieve QWR at 45° angle of incidence are excellent antireflection coatings for the underlying dielectric, semiconducting, or metallic substrate.

The characteristics of high-reflectance QWRs (at $\phi = 70°$) and HWRs (at $\phi = 45°$) using a Ag substrate coated by a dielectric thin film at several wavelengths in the visible and near IR are listed in Tables I and III. The sensitivity of these designs to errors of angle of in-

cidence, film refractive index, and film thickness has been determined and the results appear in Tables II and IV.

This work was supported by the State of Louisiana Board of Regents and the Foundation for A Better Louisiana.

This paper was presented at the 1984 Annual Meeting of the Optical Society of America, San Diego, Calif., 30 Oct.–2 Nov.

References

1. R. M. A. Azzam, A.-R. M. Zaghloul, and N. M. Bashara, "Ellipsometric Function of a Film–Substrate System: Applications to the Design of Reflection-Type Optical Devices and to Ellipsometry," J. Opt. Soc. Am. **65,** 252 (1975).
2. A.-R. M. Zaghloul, R. M. A. Azzam, and N. M. Bashara, "Design of Film–Substrate Single-Reflection Retarders," J. Opt. Soc. Am. **65,** 1043 (1975).
3. R. M. A. Azzam and M. E. R. Khan, "Single-Reflection Film–Substrate Half-Wave Retarders with Nearly Stationary Reflection Properties over a Wide Range of Incidence Angles," J. Opt. Soc. Am. **73,** 160 (1983).
4. See, for example, R. M. A. Azzam and N. M. Bashara, *Ellipsometry and Polarized Light* (North-Holland, Amsterdam, 1977), Sec. 4.3.
5. M. Born and E. Wolf, *Principles of Optics* (Pergamon, New York, 1975), p. 40.
6. If the incident light is linearly polarized at 45° azimuth with respect to the plane of incidence, so that the p and s components of the incident electric vector are equal and inphase, the p component of the electric vector of the reflected light will lead the s component by 90°, when $\rho = j$, hence the identification of the p direction as the fast axis. The $\exp(j\omega t)$ harmonic time dependence is assumed.
7. E. Ritter, "Dielectric Film Materials for Optical Applications," Phys. Thin Films **8,** 1 (1975).
8. H. K. Pulker, "Characterization of Optical Thin Films," Appl. Opt. **18,** 1969 (1979).
9. G. Hass, in *Applied Optics and Optical Engineering*, R. Kingslake, Ed. (Academic, New York, 1965), Vol. 3, Chap. 8.
10. J. H. Apfel, "Graphical Method to Design Internal Reflection Phase Retarders," Appl. Opt. **23,** 1178 (1984).
11. W. R. Hunter, "Measurement of Optical Properties of Materials in the Vacuum Ultraviolet Spectral Region," Appl. Opt. **21,** 2103 (1982).
12. S. Kawabata and M. Suzuki, "MgF_2–Ag Tunable Reflection Retarder," Appl. Opt. **19,** 484 (1980).

Meetings Schedule

OPTICAL SOCIETY OF AMERICA
1816 Jefferson Place N.W.
Washington, D.C. 20036

21–24 May 1985 CLEO 85, OSA/IEEE CONFERENCE ON LASERS AND ELECTROOPTICS, Baltimore Information: Meetings Department at OSA

10–13 June 1985 INTERNATIONAL LENS DESIGN CONFERENCE, Cherry Hill Information: Meetings Department at OSA

10–14 June 1985 SPRING CONFERENCE ON APPLIED OPTICS, Cherry Hill Information: Meetings Department at OSA

12–14 June 1985 WORKSHOP ON OPTICAL FABRICATION AND TESTING, Cherry Hill Information: Meetings Department at OSA

18–21 June 1985 INSTABILITIES AND DYNAMICS OF LASERS AND NONLINEAR OPTICAL SYSTEMS TOPICAL MEETING, Rochester Information: Meetings Department at OSA

15–17 October 1985 OPTICAL STORAGE DATA TOPICAL MEETING, Washington D.C. Information: Meetings Department at OSA

15–18 October 1985 ANNUAL MEETING OPTICAL SOCIETY OF AMERICA, Washington D.C. Information: Meetings Department at OSA

10–13 June 1986 CLEO 86, OSA/IEEE CONFERENCE ON LASERS AND ELECTROOPTICS, San Francisco Information: Meetings Department at OSA

21–24 October 1986 ANNUAL MEETING OPTICAL SOCIETY OF AMERICA, Los Angeles Information: Meetings Department at OSA